Chaos elimination in power system using synergetic control theory

1st Abdul-Basset A. Al-Hussein
Electrical Engineering Department
College of engineering, Basrah univeristy
Basrah, Iraq
abdulbasset.alhussein@gmail.com

2nd Fadhil Rahma Tahir
Electrical Engineering Department
College of engineering, Basrah univeristy
Basrah, Iraq
fadhilrahma.creative@gmail.com

3rd Olfa Boubaker
National Institute of Applied Sciences and Technology, Carthage University
Tunis, Tunisia
olfa.boubaker@insat.rnu.tn

***Abstract*—This paper puts forward the power system stability under investigation. Power system stability is critical for reliable and safe operation of the network and the protection of the power system elements. Maintaining the voltage level within normal range and the robustness against the disturbances that may lead to chaotic oscillation which finally may cause system bus voltage collapse and angle divergence. The observation of bifurcation and chaotic oscillations are analyzed for a wide range of parameters variations with the help of Lyapunov exponent, Lyapunov spectrum, and bifurcation diagram. Based on the aforementioned analysis, a robust synergetic controller design is achieved based on STATCOM and energy storage facilities to maintain the load bus voltage at the rated level and restore the synchronous operation. Simulation results confirm the effectiveness and the robustness of the proposed control scheme.**

***Index Terms*—power system stability, chaotic oscillation, chaos suppressing, synergistic control theory**

I. Introduction

Recent investigations show that the highly complex nonlinear power system can exhibit chaotic behavior leading to a voltage collapse [1], angle instability, which severely threatens the secure and stable operation of the power system and may immediately damage the whole power system and blackout [2], [3].

The chaos in power system can be triggered by parameters variations [4], noise [5], large disturbances [6] and time delay [7]. In [8] based on the fuzzy supervisor algorithm, a sliding mode control is built to ensure perfect tracking and damping chaotic oscillations in the presence of uncertainties.

A single machine infinite bus power system is studied in [9] it is reported that angle divergences due to the break of stable chaotic oscillation are causing the instability of power system, then an adaptive backstepping sliding mode controller is designed to eliminate the angle divergences and render the power system run in stable orbits. In [10] first order sliding mode controller is designed to control the chaotic behavior in an extended 4D fundamental power system. A second-order model of the power system has been analyzed in [11] to show the characteristics of chaotic oscillation, and suggest an improved adaptive sliding mode control approach based on relay characteristic function. Pole placement-based proportional integral sliding mode control is suggested to suppress the chaos in a 4D fundamental power system. Lyapunov stability theory is employed to derive sufficient conditions for asymptotic stability of the sliding manifold [12].

However, in practical applications of SMC, the design may be subjected to unwanted oscillations having finite amplitude and frequency, which is known as chattering phenomenon. Chattering is an undesirable phenomenon because it decreases the accuracy of the designed control algorithm, where it excites fast dynamics which were neglected in the ideal model, induces instability and may cause severe damage and high wear of moving mechanical parts of actuators through high frequency control effort [13]. Several solutions have been proposed to overcome this problem, all these approaches alleviate chattering to different degrees at expenses of added complexity and often robustness.

The synergetic control approach, based on the analytical design of aggregated regulators (ADAR) [14], removes chattering as a whole by the use of totally continuous control law and provides the same level of closed-loop invariance similar to the SMC. This method provides the advantages of the SMC without the chattering phenomena and its complications. The synergetic control, works on the full nonlinear system and does not need any simplification or linearization of the input-output system dynamics, as required in the traditional control theory during application [15].

Motivated by the literature survey and chaotic oscillation critical issues, this paper puts forward a robust synergetic control algorithm for chaos elimination in a 4D power system model. The controller is integrated with FACTS devices and energy storage element. There are many FACTS technologies are used to control the power system, one of the familiar is the static var compensator SVC [16] for maintaining the load bus voltage at the rated value. For better performance and faster response, the STATCOM compensator will be used in this work to support the system bus voltage stability, against the large-scale disturbances [17]. While the energy storage device will be used to recover the synchronous operation of the power system and remove the chaotic oscillation.

This paper is organized as follows. In Sec. II, the mathematical model of the chaotic power system is introduced, and the system dynamics investigated to reveal the system behavior which shows a chaotic state at parameters variation. In Sec. III, the synergetic controller design is provided and the dynamics of the STATCOM compensator and the energy storage device are introduced. In Sec. IV, two simulation examples were provided to reveal the controller effectiveness and robustness. Then general conclusions and discussion are given in Sec. V.

II. Mathematical Model

The power system scheme is shown in Fig. 1, which is a benchmark model introduced in [16], [18], for studying the voltage stability. The model consists of three buses, the first bus is the generator bus and the second bus is the load bus while the third bus is the generator slack bus. The load bus constituted from induction motor in parallel with constant PQ load. The full power system dynamical model can be written as follows:

$$\begin{cases} \dot{\delta}_m & = \omega, \\ M\dot{\omega} & = -d_m\omega + P_m + E_m Y_m V \sin(\delta - \delta_m - \theta_m) \\ & +E_m^2 Y_m \sin\theta_m, \\ K_{qw}\dot{\delta} & = -K_{qv2}V^2 - K_{qv}V + E_0' Y_0' V \cos(\delta + \theta_0') \\ & +E_m Y_m V \cos(\delta - \delta_m + \theta_m) - (Y_0' \cos\theta_0' \\ & +Y_m \cos\theta_m) V^2 - Q_0 - Q_1, \\ TK_{qw}K_{pv}\dot{V} & = K_{pw}K_{qv2}V^2 + (K_{pw}K_{qv} - K_{qw}K_{pv}) V \\ & +K_{qw}\big(-E_0' Y_0' V \sin(\delta + \theta_0') \\ & -E_m Y_m V \sin(\delta - \delta_m + \theta_m) \\ & +(Y_0' \sin\theta_0' + Y_m \sin\theta_m) V^2 - P_0 - P_1\big) \\ & -K_{pw}\big(E_0' Y_0' V \cos(\delta + \theta_0') \\ & +E_m Y_m V \cos(\delta - \delta_m + \theta_m) \\ & -(Y_0' \cos\theta_0' + Y_m \cos\theta_m) V^2 - Q_0 - Q_1\big) \end{cases} \tag{1}$$

where δ_m represents the generator angle, ω is the frequency deviation. M is the inertia of the generator, d_m represents the damping coefficient and P_m is the mechanical input power. Y_m and θ_m are the admittance and the impedance angle of the transmission line, respectively. E_m refers to the generator voltage magnitude. V and δ stand for the load voltage magnitude and the phase angle, respectively. P_1 and Q_1 are the real and reactive power of the constant PQ load, respectively. The induction motor real power and reactive power are defined as P_0 and Q_0, respectively. And its constants are given by K_{pv}, K_{pw}, K_{qv}, K_{qw} and K_{qv2}. E_0', Y_0' and θ_0' are Thevenin equivalent circuit parameters.

To investigate the power system dynamical behavior, the input mechanical power P_m, will be considered as a bifurcation parameter. The system parameters are adapted from [16] as follow: $E_{\rm m} = 1.05$, $Y_{\rm m} = 5.0$, $\theta_{\rm m} = 0$, $E_0' = 20$, $Y_0' = 0.1665$, $\theta_0' = 0$, $d_{\rm m} = 0.05$, $M = 0.01464$, $K_{\rm pw} = 0.4$, $K_{\rm qv2} = 2.1$, $K_{\rm qw} = -0.03$, $K_{\rm qv} = -2.8$, $K_{\rm pv} = 0.3$, $T = 8.5$, $P_0 = 0.6$, $Q_0 = 1.3$, $P_1 = 0$, $Q_1 = 2.9$. All parameters values are in per unit except θ_m and θ_m' are in rad. The initial conditions of the system are considered as $[\delta_m(0), \omega(0), \delta(0), V(0)]^T = [0.29, 0.2, 0.23, 0.8]^T$. Using the local maximum method and changing the bifurcation parameter P_m in the range of [1.096,1.102], the bifurcation diagram of (1) state ω can be drawn as shown in Fig. 3. The bifurcation diagram reveals that when $P_m \in [1.0961.0985]$, the power system behaves periodically. While a period doubling bifurcation occurs in the range $P_m \in [1.09851.1006]$. And in the interval $P_m \in [1.10061.102]$ the power system states become chaotic and follow a period doubling root to chaos. The Lyapunov spectrum can show the stated dynamics as shown in Fig. 4. The time domain waveforms and the phase plane chaotic attractor of the power system at $P_m = 1.102$ are shown in Fig. 5 and Fig. 6, respectively. These figures show that the system is so aperiodic and has an irregular oscillation. All the aforementioned analyses reveal the chaotic existence in the power system. The chaos in the power system results in voltage collapse and then may lead to unwanted blackout. So, it is important to design a robust control algorithm to suppress the chaotic states of the power system as will be done in the next section.

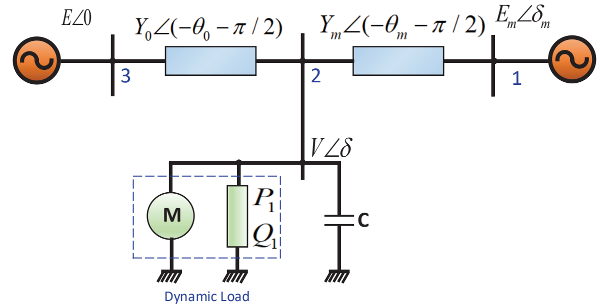

Fig. 1. The power system model (1) under investigation.

III. Synergetic Controller Design

To implement the synergetic controller, a method based on integrating the synergetic control theory with the STATCOM and energy storage device are presented. The system dynamics of the STATCOM and energy storage device are given in (2) [17], [19]:

$$\begin{cases} \dot{i}_{stat} & = -\frac{1}{T_{stat}} i_{stat} + \frac{K_{stat}}{T_{stat}} u_{stat} \\ \dot{P}_{es} & = -\frac{1}{T_{es}} P_{es} + \frac{K_{es}}{T_{es}} u_{es} \end{cases} \tag{2}$$

where i_{stat} denotes the STATCOM compensator current, K_{stat} and T_{stat} represent the gain and time constant of the STATCOM, respectively. u_{stat} refers to the STATCOM input control. P_{es} denotes the energy storage device real power, K_{es} and T_{es} represent the gain and time constant of the energy storage device, respectively. u_{es} refers to the energy storage input control. The complete controlled power system circuit diagram is shown in Fig. 2. The energy storage device is located on bus 1 to damp out the oscillation, while the STATCOM is connected to the local load bus 2 to maintain

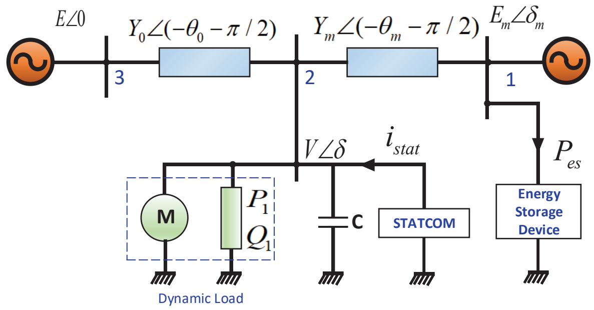

Fig. 2. The complete controlled power system (3) circuit diagram.

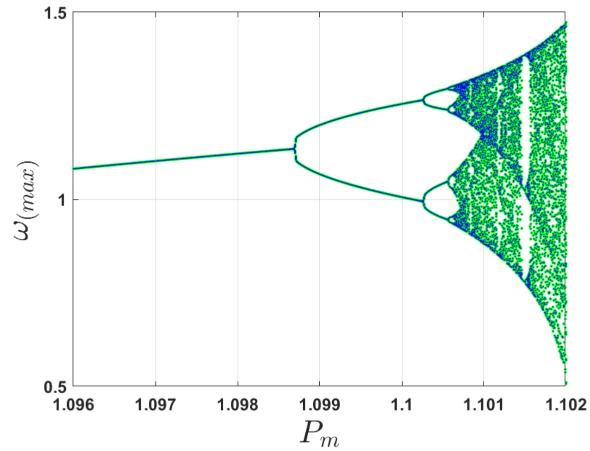

Fig. 3. Bifurcation diagram of the chaotic power system (1) for the system state ω varying with P_m.

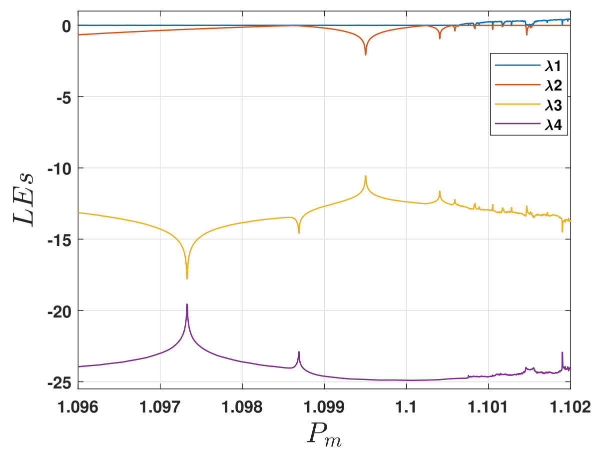

Fig. 4. Lyapunov spectrum for the power system (1) varying with P_m.

the rated voltage level. To derive the mathematical model of the controlled power system, combine (1) with (2) yields a six-dimensional power system model (3):

$$\begin{cases} \dot{\delta}_m &= \omega = f_1, \\ \dot{\omega} &= \frac{1}{M}\left[-d_m\omega + P_m + E_m Y_m V \sin\left(\delta - \delta_m - \theta_m\right) \right. \\ & \left. + E_m^2 Y_m \sin\theta_m - P_{es}\right] = f_2, \\ \dot{P}_{es} &= -\frac{1}{T_{es}} P_{es} + \frac{K_{es}}{T_{es}} u_{es} \\ \dot{\delta} &= \frac{1}{K_{qw}}\left[-K_{qv2}V^2 - K_{qv}V + E_0' Y_0' V \cos\left(\delta + \theta_0'\right) \right. \\ & + E_m Y_m V \cos\left(\delta - \delta_m + \theta_m\right) - \left(Y_0' \cos\theta_0' \right. \\ & \left. \left. + Y_m \cos\theta_m\right) V^2 - Q_0 - Q_1 - Q_{stat}\right] = f_3, \\ \dot{V} &= \frac{1}{T K_{qw} K_{pv}}\left[K_{pw}K_{qv2}V^2 + \left(K_{pw}K_{qv} - K_{qw}K_{pv}\right) V \right. \\ & + K_{qw}\left(-E_0' Y_0' V \sin\left(\delta + \theta_0'\right) \right. \\ & - E_m Y_m V \sin\left(\delta - \delta_m + \theta_m\right) \\ & \left. + \left(Y_0' \sin\theta_0' + Y_m \sin\theta_m\right) V^2 - P_0 - P_1\right) \\ & - K_{pw}\left(E_0' Y_0' V \cos\left(\delta + \theta_0'\right) \right. \\ & + E_m Y_m V \cos\left(\delta - \delta_m + \theta_m\right) \\ & - \left(Y_0' \cos\theta_0' + Y_m \cos\theta_m\right) V^2 - Q_0 - Q_1 \\ & \left. \left. - Q_{stat}\right)\right] = f_4, \\ \dot{i}_{stat} &= -\frac{1}{T_{stat}} i_{stat} + \frac{K_{stat}}{T_{stat}} u_{stat} \end{cases} \tag{3}$$

where Q_{stat} refers to reactive power provided by the STATCOM, which can be written as $Q_{stat} = i_{stat}V$.

Defining the following transform $x_1 = \delta_m$, the first three equations of controlled system (3) can be written as:

$$\begin{cases} \dot{x}_1 &= x_2 \\ \dot{x}_2 &= x_3 \\ \dot{x}_3 &= \dot{f}_2 \end{cases} \tag{4}$$

Then define the synergetic control macro variable for the first auxiliary system (4) as follows:

$$\psi_1 = x_3 + k_2 x_2 + k_1 x_1 \tag{5}$$

and this macro variable (5) will be evolved according to the following dynamical constrain (6):

$$\dot{\psi}_1 + \frac{1}{T_1}\psi_1 = 0 \tag{6}$$

To achieve the second control objective, maintaining the load bus voltage level at the rated voltage, assume the following transform $x_4 = V - 1$, the last two equations of controlled system (3) can be written as:

$$\begin{cases} \dot{x}_4 &= x_5 \\ \dot{x}_5 &= \dot{f}_4 \end{cases} \tag{7}$$

For the second auxiliary system (7), assume the macro variable and the evolution constrain as defined in (8) and (9), respectively:

$$\psi_2 = x_5 + k_3 x_4 \tag{8}$$

$$\dot{\psi}_2 + \frac{1}{T_2}\psi_2 = 0 \tag{9}$$

By solving the dynamical constrains (6) and (9) using the defined auxiliary systems (4) and (7), for u_{stat} and u_{es}, these two input controls can be written as follows:

$$\begin{cases} u_{es} & = \frac{T_{es}M}{K_{es}}\left[f_5 + k_2 x_3 + k_1 x_2 + \frac{1}{T_1}\psi_1\right] \\ \\ u_{stat} & = \frac{-T_{stat}TK_{qw}K_{pv}}{K_{statK_{pw}V^2}}\left[f_6 + k_3 x_5 + \frac{1}{T_2}\psi_2\right] \end{cases} \tag{10}$$

where

$$\begin{cases} f_5 & = \frac{-1}{M}\left[d_m f_2 - E_m Y_m f_4 \sin(\delta - \delta_m - \theta_m)\right. \\ & \left. - E_m Y_m V(f_3 - f_1)\cos(\delta - \delta_m - \theta_m) - \frac{1}{T_{es}}P_{es}\right], \\ \\ f_6 & = \frac{-1}{TK_{qw}K_{Kpv}}\left[-2K_{pw}K_{qv2}Vf_4 - (K_{pw}K_{qv}\right. \\ & -K_{qw}K_{pv})f_4 - K_{qw}f_7 + K_{pw}f_8 - 2K_{pw}i_{stat}Vf_4 \\ & \left.\frac{i_{stat}K_{pw}V^2}{T_{stat}}\right], \\ \\ f_7 = & -E_0'Y_0'\left[f_4\sin(\delta + \theta_0') + Vf_3\cos(\delta + \right. \\ & \left.\theta_0')\right] - E_{\mathrm{m}}Y_{\mathrm{m}}\left[f_4\sin(\delta - \delta_{\mathrm{m}} + \theta_{\mathrm{m}}) + \right. \\ & \left.V(f_3 - f_1)\cos(\delta - \delta_{\mathrm{m}} + \theta_{\mathrm{m}})\right] + 2\left(Y_0'\sin\theta_0' + \right. \\ & \left.Y_{\mathrm{m}}\sin\theta_{\mathrm{m}}\right)Vf_4, \\ \\ f_8 = & E_0'Y_0'\left[f_4\cos(\delta + \theta_0') - Vf_3\sin(\delta + \theta_0')\right] + \\ & E_{\mathrm{m}}Y_{\mathrm{m}}\left[f_4\cos(\delta - \delta_{\mathrm{m}} + \theta_{\mathrm{m}}) - V(f_3 - f_1)\right. \\ & \left.\sin(\delta - \delta_{\mathrm{m}} + \theta_{\mathrm{m}})\right] - 2\left(Y_0'\cos\theta_0' + \right. \\ & \left.Y_{\mathrm{m}}\cos\theta_{\mathrm{m}}\right)Vf_4 \end{cases} \tag{11}$$

Theorem 1. *Consider the nonlinear chaotic power system* (1)*, the system will converge to the invariant manifolds* $\psi_1 = 0$ *and* $\psi_2 = 0$*, under the action of the control laws* (14)*.*

Proof: Define a Lyapunov candidate function as

$$V = \frac{1}{2}(\psi_1^2 + \psi_2^2) \tag{12}$$

then the time derivative of V is:

$$\dot{V} = (\psi_1\dot{\psi_1} + \psi_2\dot{\psi_2}) \tag{13}$$

substituting (6) and (9) into (13):

$$\begin{cases} \dot{V} & = \psi_1(-\frac{1}{T_1}\psi_1) + \psi_2(-\frac{1}{T_2}\psi_2), \\ & = -\left[\frac{1}{T_1}\psi_1^2 + \frac{1}{T_2}\psi_2^2\right] \end{cases} \tag{14}$$

Therefore, $\dot{V} \leq 0$.
And this is complete the proof. ■

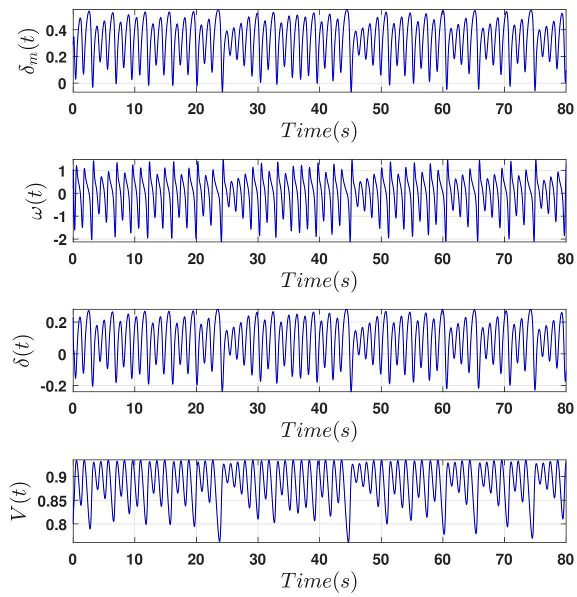

Fig. 5. Time responses for the chaotic power system (1).

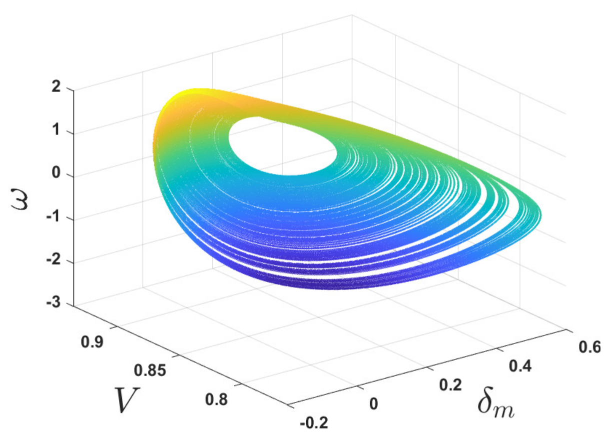

Fig. 6. Phase diagram of the chaotic power system (1).

IV. Simulation Results

Two illustrative scenarios are considered to show the effectiveness, the robustness, and the superiority of the designed controller in eliminating the chaos in the power system. The controller parameters are selected as $k_1 = 25$, $k_2 = 10$, $k_3 = 5$, $T_1 = T_2 = 0.2$, $T_{stat} = 0.01$, $K_{stat} = 1$, $T_{es} = 1$, and $K_{es} = 1$.

In the first scenario, the controller is implemented at the beginning time of the simulation and the power system is in the chaotic state where $P_m = 1.102$.

The time waveforms of the state variables under the proposed controller are displayed in Fig. 7, it is clear that the system states responses derived to the normal state without

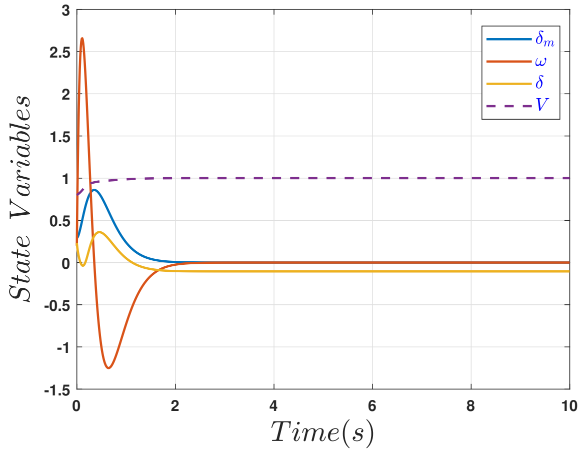

Fig. 7. Controlled system (3) time responses with control in action at t=0 [Sec].

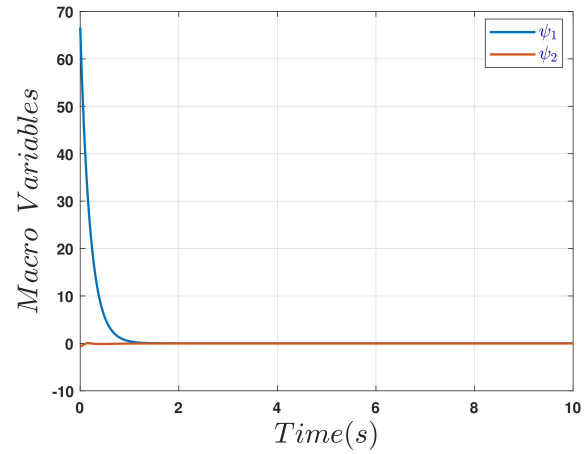

Fig. 9. The synergetic macro variables of the proposed controller.

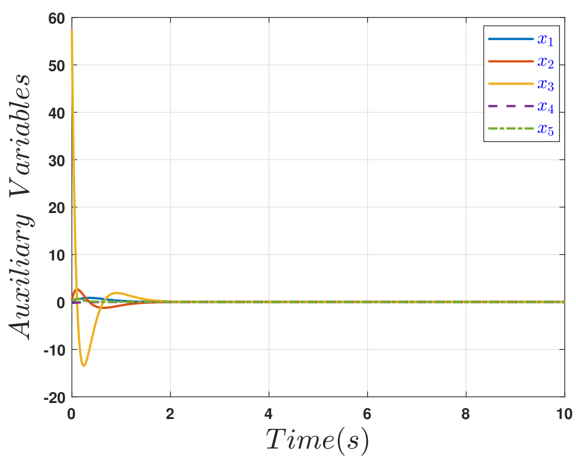

Fig. 8. The auxiliary systems states time waveforms.

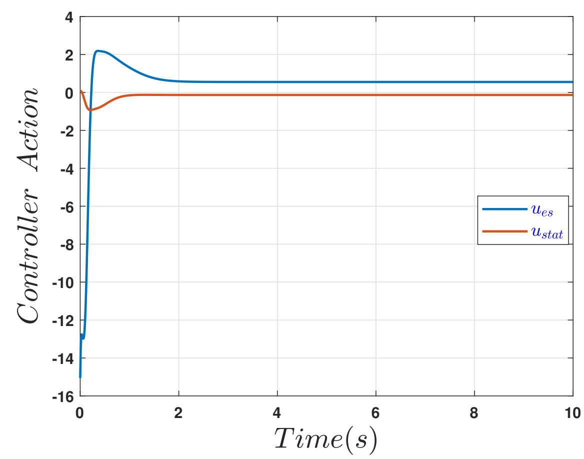

Fig. 10. Control inputs for the chaotic power system (1).

chaotic oscillation and settle down to the equilibrium state. Fig. 8 and Fig. 9 show the auxiliary variables and the synergetic macro variables ψ_1 and ψ_2, respectively. The system reaches the invariant manifold as required under the synergetic control algorithm. The controller action and the control state time series are depicted in Fig. 10 and Fig. 11, it is clear that the control actions are chattering free and smooth. And this is rendering the controller feasible for practical applications.

In the second scenario, the system works in a chaotic oscillation state then the controller is applied at an arbitrary time point. The time response waveforms of the system state variable are given in Fig. 12 where the control applied at $t = 175\ (s)$. The trajectories evolution is shown in Fig. 13, obviously the power system dynamics leave the chaotic attractor after applying the synergetic controller and then follow the red line in Fig. 13, to settle down finally to the equilibrium state.

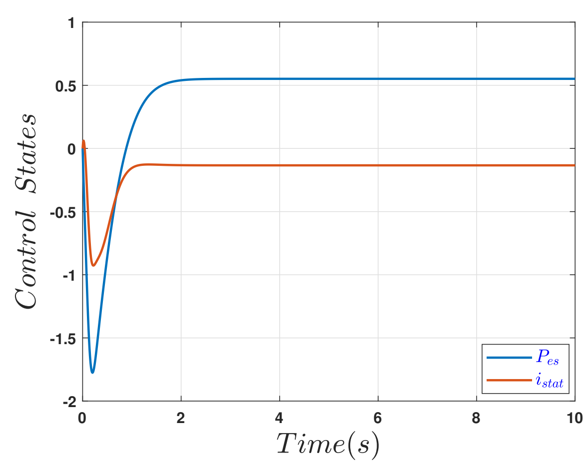

Fig. 11. Active power absorbed by the energy storage device and the STATCOM compensator current.

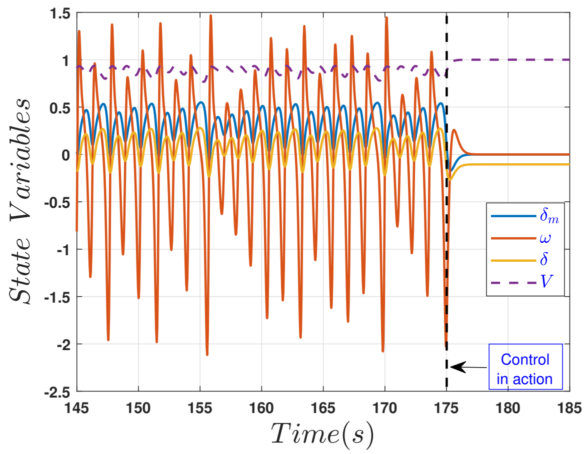

Fig. 12. Controlled system (3) time responses with control in action at $t = 175$ (s).

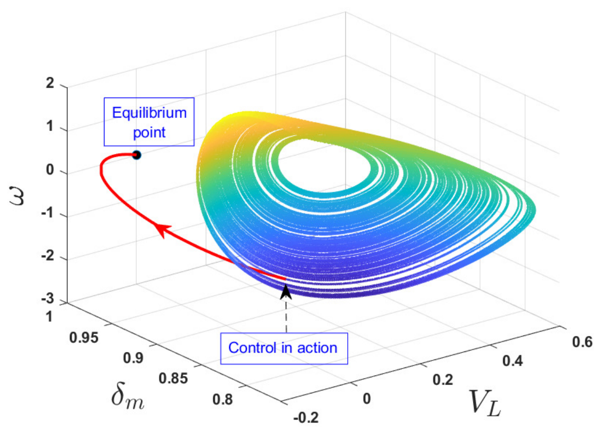

Fig. 13. Phase diagram of the controlled power system (3) with control in action at $t = 175$ (s). The red line represents the trajectory leaving the chaotic attractor.

V. Conclusion

In this paper, a synergetic control theory has been employed to design an effective and a robust controller for chaos suppressing in a power system. The design integrated the synergetic theory, along with the STATCOM compensator and the energy storage device. The resulted controller, successfully achieved the control objectives with fast response, chattering free control actions and effective recovery of the system states to the synchronous operation. Lyapunov stability has been used to show the whole system stability and prove the convergence of the synergetic macro variables, to the invariant manifolds through the selected dynamical constrain. Numerical simulation results reveal the effectiveness and the superiority of the designed controller when applied to the chaotic power system.

References

[1] Z. Hui, M. Ya-Jun, L. Si-Jia, G. Shi-Gen, and Z. Dan, "Controlling chaos in power system based on finite-time stability theory," *Chinese Physics B*, vol. 20, no. 12, p. 120501, 2011.

[2] P. C. Gupta, A. Banerjee, and P. P. Singh, "Analysis of global bifurcation and chaotic oscillation in distributed generation integrated novel renewable energy system," in *2018 15th IEEE India Council International Conference (INDICON)*. IEEE, 2018, pp. 1–5.

[3] W. Qiao, G. K. Venayagamoorthy, and R. G. Harley, "Missing-sensor-fault-tolerant control for sssc facts device with real-time implementation," *IEEE Transactions on Power Delivery*, vol. 24, no. 2, pp. 740–750, 2009.

[4] X. Chen, W. Zhang, and W. Zhang, "Chaotic and subharmonic oscillations of a nonlinear power system," *IEEE Transactions on Circuits and Systems II: Express Briefs*, vol. 52, no. 12, pp. 811–815, 2005.

[5] D. Wei and X. Luo, "Noise-induced chaos in single-machine infinite-bus power systems," *EPL (Europhysics Letters)*, vol. 86, no. 5, p. 50008, 2009.

[6] Y. Yu, H. Jia, P. Li, and J. Su, "Power system instability and chaos," *Electric power systems research*, vol. 65, no. 3, pp. 187–195, 2003.

[7] M. Mei-Ling and M. Fu-Hong, "Bifurcation behavior and coexisting motions in a time-delayed power system," *Chinese Physics B*, vol. 24, no. 3, p. 030501, 2015.

[8] A. S. A. Abadi and S. Balochian, "Chaos control of the power system via sliding mode based on fuzzy supervisor," *International Journal of Intelligent Computing and Cybernetics*, 2017.

[9] F. Min, Y. Wang, G. Peng, E. Wang, and J. A. Auth, "Bifurcations, chaos and adaptive backstepping sliding mode control of a power system with excitation limitation," *Aip advances*, vol. 6, no. 8, p. 085214, 2016.

[10] M. Kumar and P. P. Singh, "Chaos control of an extended four dimensional fundamental power system using sliding mode control," in *2018 5th IEEE Uttar Pradesh Section International Conference on Electrical, Electronics and Computer Engineering (UPCON)*. IEEE, 2018, pp. 1–6.

[11] Z. Shang, Y. Yu, and Y. Li, "Adaptive sliding mode control of chaotic oscillation in power system based on relay characteristic function," in *2020 IEEE/IAS Industrial and Commercial Power System Asia (I&CPS Asia)*. IEEE, 2020, pp. 1012–1016.

[12] M. Kumar and P. P. Singh, "Chaos control of a four-dimensional fundamental power system using pole placement-based proportional integral sliding mode control," *International Journal of Automation and Control*, vol. 13, no. 6, pp. 679–697, 2019.

[13] S. Yu, X. Yu, B. Shirinzadeh, and Z. Man, "Continuous finite-time control for robotic manipulators with terminal sliding mode," *Automatica*, vol. 41, no. 11, pp. 1957–1964, 2005.

[14] A. Kolesnikov, G. Veselov, A. Kolesnikov *et al.*, "Modern applied control theory: synergetic approach in control theory," *TRTU, Moscow, Taganrog*, pp. 4477–4479, 2000.

[15] M. P. Lazarević, "Elements of mathematical phenomenology of self-organization nonlinear dynamical systems: Synergetics and fractional calculus approach," *International Journal of Non-Linear Mechanics*, vol. 73, pp. 31–42, 2015.

[16] J. WANG and C. LIU, "Synergetic control method for four-dimensional chaotic power system," 2020.

[17] S. Li, Q. Zhao, C. Chen, and Y. Xu, "A comparative study on voltage stability bifurcation control ability of svc and statcom," in *2012 China International Conference on Electricity Distribution*. IEEE, 2012, pp. 1–4.

[18] I. Dobson and H.-D. Chiang, "Towards a theory of voltage collapse in electric power systems," *Systems & Control Letters*, vol. 13, no. 3, pp. 253–262, 1989.

[19] J. Fang, W. Yao, Z. Chen, J. Wen, and S. Cheng, "Design of anti-windup compensator for energy storage-based damping controller to enhance power system stability," *IEEE Transactions on Power Systems*, vol. 29, no. 3, pp. 1175–1185, 2013.